

# Minimization of total harmonic distortion in neutral point clamped multilevel inverter using grey wolf optimizer

Fahmi Ahyar Izzaqi, Novie Ayub Windarko, Ony Asrarul Qudsi

Electrical Engineering Department, Politeknik Elektronika Negeri Surabaya, Surabaya, Indonesia

## Article Info

### Article history:

Received Mar 18, 2022

Revised May 22, 2022

Accepted Jun 15, 2022

### Keywords:

Grey wolf optimizer

Modified PWM

Multilevel inverter

Optimization algorithm

Total harmonic distortion

## ABSTRACT

The inverter has been attracting researchers for their application in renewable energy. So far, multilevel inverter is considered as low distortion class, which produces multilevel output voltage imitating a pure sine waveform. However, the needs for free distortion of output voltage have been motivating to improve multilevel pulse width modulation PWM generation method. In this paper, the modified PWM technique is proposed to reduce the voltage total harmonics distortion (THD) of multilevel inverter. This modulation technique is then applied to control a single-phase three-level neutral point clamped multilevel inverter (NPC-MLI). Grey wolf optimizer (GWO) algorithm is utilized to generate optimal amplitude and phase shift of modified reference signal. The GWO algorithm is then compared with other optimization algorithms such as differential evolution (DE), human psychology optimization (HPO), and particle swarm optimization (PSO) to evaluate their performance in harmonic minimization. The performance of the proposed work is validated through simulation and experimentation on a prototype. The results show that the modified PWM technique optimized with GWO can reduce THD on NPC-MLI output voltage.

*This is an open access article under the [CC BY-SA](#) license.*



## Corresponding Author:

Fahmi Ahyar Izzaqi

Electrical Engineering Department, Politeknik Elektronika Negeri Surabaya

ITS Raya st, Keputih, Sukolilo, Surabaya, East Java 60111, Indonesia

Email: fahmizzaqi@pe.student.pens.ac.id

## 1. INTRODUCTION

Since several decades ago, multilevel inverter multilevel inverter (MLI) has been attracting to convert direct current DC voltage to alternating current AC voltage in renewable energy applications [1]. The MLI are widely used as voltage converters from renewable energy source such as solar panels, wind turbines and others, to supply electricity to AC loads in stand-alone systems [2] or to the grid-connected [3]. High efficiency power conversion systems are expected to deliver high performance by reducing conduction losses in the switching process and reducing total harmonics distortion total harmonics distortion (THD) [4]. So far, MLI is well known has low voltage distortion and can operate at high power and high switching frequency [5]. Under ideal condition, the MLI should provide pure sine wave for electric loads. The MLI can produce staircase output voltage which close to a sinewave form. However, the MLI's staircase output voltage is non ideal sine wave and still contains harmonics due to the switching pattern generation [6]. To overcome this issue, many type of MLI has been developed includes cascaded H-Bridge MLI, flying capacitor MLI, and neutral point clamped multilevel inverter neutral point clamped multilevel inverter (NPC-MLI) [7]. Due to MLI circuit complexity, several researchers have proposed to reduce the number of MLI's components [8]. Nevertheless, the NPC MLI has advantages of easy control and low cost hardware implementation among the MLIs [9].

Beside the topological solutions, reducing THD of output voltage by generating proper switching pattern modulation is also a hot issue of research in MLIs [10], such as multi-carrier PWM [11], selective harmonic elimination pulse width modulation PWM [12], and space vector modulation [13]. Many studies have been performed to reduce the harmonics of the output voltage of a MLI [14]. Several modulation techniques have been reported to selectively eliminate lower order harmonics of MLIs staircase output voltage [15]. Moreover, injection techniques are also common by injecting various reference signals to modulated signal [16]. Many researchers have proposed new injection techniques such as third harmonic injection PWM [17], third harmonic injection space vector PWM [18], and generalized discontinuous PWM [19]. Each injection technique has shown specific and various THD value of the output voltage. Recently, several modulation techniques to minimize the THD of MLI output voltage was improved by utilizing metaheuristic algorithm [20]. Improved whale optimization algorithm is used to optimize the switching angles of a single phase 5 and 7 level multilevel inverters (MLIs) [21]. Grasshopper optimization algorithm is used for optimizing switching angles applied to a three-phase 7-level cascaded H-bridge multilevel inverter [22]. To minimize the THD in cascaded MLI, the hyper-spherical search algorithm is used [23]. The use of metaheuristic algorithm to optimize injection techniques in NPC-MLI is proposed, such as genetic algorithm (GA) [24] and differential evolution (DE) [25]. However, drawbacks in metaheuristic algorithms can restrict the minimization of THD. For example, insufficient local search ability, slow convergence rate and premature convergence are main limitations associated with GA [26]. Also, the DE performance are fully influenced by the parameter of scaling factor and the crossover rate [27]. So, the determination of those control parameters is significant in the mutation and crossover operations. Hence, to improve the THD minimization, researchers have been promoting novel modulation and higher performance optimizer algorithms.

Based on the above mentioned, this paper is intensively proposed a low-cost approach to reduce THD by injection technique to modulated signal for NPC-MLI. This paper also provides discussion and analysis of the injected PWM optimization using grey wolf optimizer GWO. GWO is a meta-heuristic method that is guaranteed to be very efficient and effective when applied to solve constrained problem or unconstrained problem, fast to achieve convergence, and avoid local optimization [28]. GWO imitates the hunting strategy and social hierarchy of grey wolves. GWO has four hunting strategies of searching, encircling, hunting, and attacking to achieve the prey location. The social hierarchy consists of alpha, beta, delta, and omega wolves. Alpha, beta, and delta wolf means the first, second and third best solution for optimization respectively. Omega wolves means worse solutions than delta wolf. GWO is used to find the best injected signal parameters of frequency, amplitude, and phase shift. The PWM modulation techniques is applied to NPC-MLI, then tested in PSIM software simulation and verified under experimental works.

## 2. RESEARCH METHOD

### 2.1. Neutral point clamped–multilevel inverter

The inverter is a device that converts a DC voltage into AC voltage. Conventional inverters typically have three output voltage levels, +V<sub>dc</sub>, -V<sub>dc</sub>, and zero. Multilevel inverter is a type of inverter that can generate multilevel voltage and current levels. NPC-MLI also known as diode clamped multilevel inverter (DC-MLI). The NPC-MLI consists of two pairs of switches in series (upper and lower), parallel to two capacitors in series where the anode of the upper diode is connected to the midpoint of the capacitor and the cathode to the midpoint of the top half diodes of the switch pair. The cathode of the lower diode is connected to the mid-point of the capacitor which enables the main DC voltage to be divided into smaller voltages (1/2 VDC). The mid-point of the two capacitors can be defined as the “neutral point” [24]. Figure 1 shown a schematic of single phase three level neutral point clamped multilevel inverter. The NPC-MLI has (m-1) the number of DC capacitors, (m-1)\*(m-2) the number of clamping diodes, and 2\*(m-1) the number of switching components per phase, *m* is the level of the multilevel inverter.

### 2.2. Modified PWM technique

The switching process is the cause of the THD of the NPC-MLI output voltage. As a result, an appropriate modulation technique is required to reduce the effect of harmonic distortion. In this paper, a modified PWM technique is proposed. The conventional modulation technique that is commonly used is sinusoidal pulse width modulation SPWM. This modulation technique is formed by comparing the sine reference signal with the triangular carrier signal. NPC-MLI requires a few semiconductor components so that more than one reference signal and a carrier signal are required.

The modified PWM techniques can be observed in Figure 2. The modified reference signal is produced by combining two signals of reference signal and injected signal. The reference signal is sinus waveform with fundamental frequency, and the injected signal has designated value of frequency, phase shift, and amplitude. The injected signal can be single or multiple signals. The mathematical equations for signals are as:

$$V_s(t) = A_1 \sin 2\pi f_1 t \quad (1)$$

$$V_i(t) = \sum_{n=2}^{\infty} A_n (\sin 2\pi f_n t + \theta_n) \quad (2)$$

Which  $V_s$  is reference signal and  $V_i$  are injected signals.

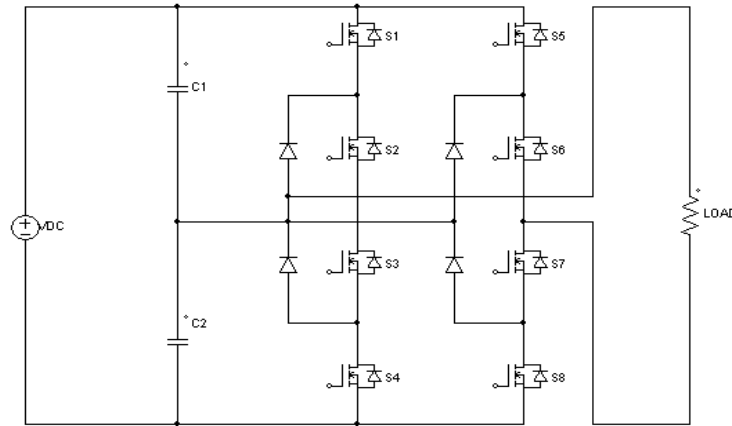


Figure 1. Schematic of single phase three level NPC-MLI

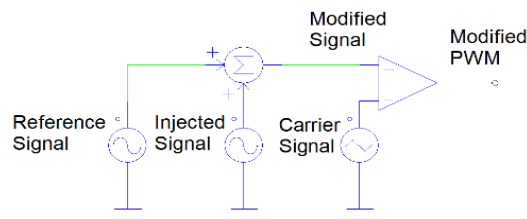


Figure 2. Schematic of the modified

In (1) is a sinusoidal reference one that has an amplitude of 1 and fundamental frequency of 50 Hz. in (2) is signal of injected signal. The injected signal aims to modify the reference waveform. This signal has the value of amplitude ( $A_n$ ), frequency ( $f_n$ ) and phase shift ( $\theta_n$ ), which their best value will be found through the Grey Wolf Optimizer tracking process. The two signals are added, resulting in the mathematical in (3), and for example in (4).

$$V_{ms}(t) = A_1 \sin 2\pi f_1 t + \sum_{n=2}^{\infty} A_n (\sin 2\pi f_n t + \theta_n) \quad (3)$$

$$V_{ms}(t) = \sin 2\pi 50t + 0.1 \{\sin 2\pi 750t + 180^\circ\} \quad (4)$$

Which  $V_{ms}$  is modified sinusoidal reference signal.

Figure 3 illustrates the process of generating a modified PWM signal using in 1-3. Figure 3(a) shows a sine reference wave one based on in (1), with an amplitude of 1 and a fundamental frequency of 50 Hz. Also, Figure 3(b) shows an injected signal waveform based on in (2) which has an amplitude of 0.1, a frequency of 750 Hz, and a phase shift of 180 degrees. Figure 3(c) shows both signals are combined and generate a modified reference signal that will be compared to the triangular carrier signal and form a modified PWM.

### 2.3. Grey wolf optimizer for minimization THD

The grey wolf optimizer (GWO) is a meta-heuristic method for finding optimal solutions of numerical problems. This method was adapted from the hunting behaviour of a herd of grey wolves. A wolf pack has a division of the leadership hierarchy, namely alpha ( $\alpha$ ), beta ( $\beta$ ), delta ( $\delta$ ) and omega ( $\omega$ ). Alpha is the best solution and as the leader of the herd. Beta and delta are the second and the third best solution that stands for alpha. While omega is the rest of the herd [20]. Figure 4(a) shows the hunting behaviour of grey wolves and Figure 4(b) shows flowchart of the GWO algorithm.

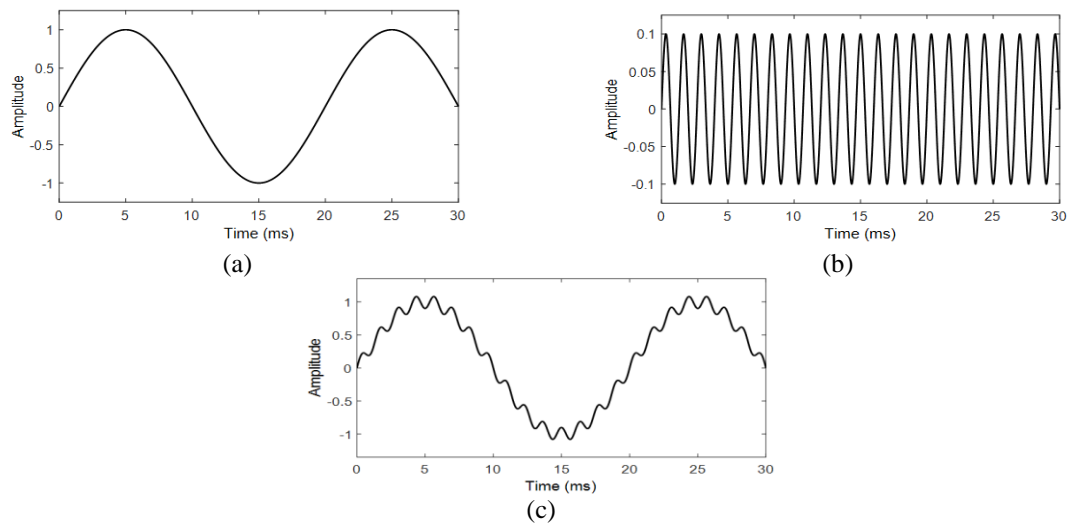
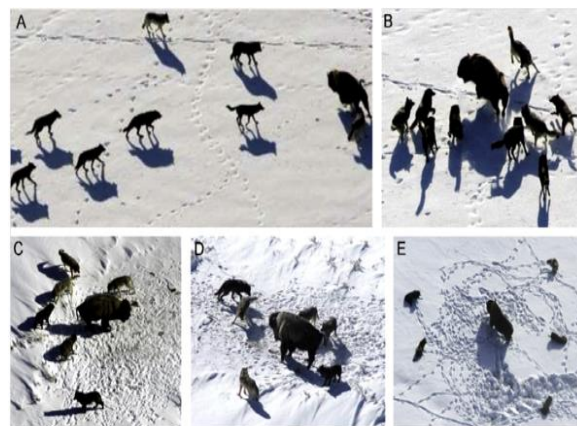
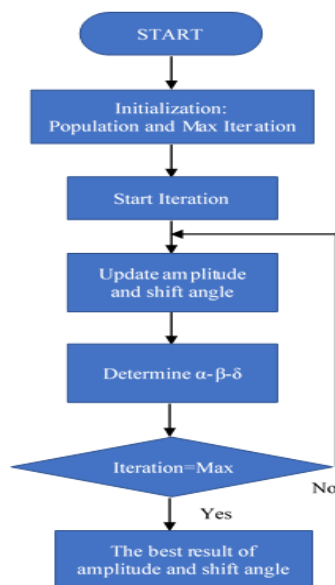


Figure 3. Modified reference signal generation scheme: (a) sinusoidal reference, (b) injected signal, and (c) modified reference signal



(a)



(b)

Figure 4. Illustration of GWO algorithm: (a) the hunting behavior of grey wolves [28] and (b) GWO flowchart

Based on the behaviour of wolf hunting, this method consists of 4 steps for obtaining the best solution. These steps include tracking, encircling, hunting, and attacking. It has been adapted as a method to find the best parameters in the modified PWM modulation process. The process of this algorithm can be explained as:

– Searching

Searching is the first step for a pack of wolves to hunt prey. In this step all members of the herd will spread out in a certain area to find prey. In its application to modified PWM, this step is carried out by giving the initial value of the solution or the initial position of the herd randomly with a certain range of the parameters of frequency, amplitude, and phase shift. After spreads, each member's position in this herd will be evaluated.

– Encircling

Encircling can be illustrated as a step to surround prey. Each member of the flock will keep their distance and move progressively closer to the prey. This siege will be led by alpha ( $\alpha$ ) and assisted by beta ( $\beta$ ) and delta ( $\delta$ ). While the movement of omega will follow alpha, beta and delta. This step is adapted into the following.

$$\vec{D} = |\vec{C} \cdot \vec{X}_p(t) - \vec{X}_p(t)| \quad (5)$$

$$\vec{X}(t+1) = \vec{X}_p(t) - \vec{A} \cdot \vec{D} \quad (6)$$

In the equation,  $t$  is the current iteration value. While  $D$ ,  $A$ , and  $C$  are vector coefficients.  $X_p$  is the position vector of the prey and  $X$  is the position vector of the wolf. Vector values  $A$  and  $C$  can be calculated using the following equation.

$$\vec{A} = 2\vec{a} \cdot \vec{r}_1 - \vec{a} \quad (7)$$

$$\vec{C} = 2 \cdot \vec{r}_2 \quad (8)$$

The value of  $a$  decreases linearly from 2 to 0 according to the iteration value. While the values of  $r_1$  and  $r_2$  are generated randomly.

– Hunting

In an abstract search space, the optimal location (prey) is unknown. Alpha is the best candidate solution, whereas beta and delta have better insight about potential prey locations. The first three best solutions obtained should update their positions accordingly to the best search agent positions. The following formula is proposed.

$$\vec{D}_\alpha = |\vec{C}_1 \cdot \vec{X}_\alpha - \vec{X}|, \vec{D}_\beta = |\vec{C}_2 \cdot \vec{X}_\beta - \vec{X}|, \vec{D}_\delta = |\vec{C}_3 \cdot \vec{X}_\delta - \vec{X}| \quad (9)$$

$$\vec{X}_1 = \vec{X}_\alpha - \vec{A}_1 \cdot \vec{D}_\alpha, \vec{X}_2 = \vec{X}_\beta - \vec{A}_2 \cdot \vec{D}_\beta, \vec{X}_3 = \vec{X}_\delta - \vec{A}_3 \cdot \vec{D}_\delta \quad (10)$$

$$\vec{X}_{(t+1)} = \frac{\vec{X}_1 + \vec{X}_2 + \vec{X}_3}{3} \quad (11)$$

– Attacking

Attacking the prey is the final step in the wolf hunting process. The attacking process is carried out when the prey has stopped moving. In its application to modified PWM optimization, this process is carried out when the solution results from each member of the herd has reached the convergence value. This value will then be performed as a best solution. Illustration of the grey wolf hunting process shown and the flowchart of the GWO algorithm is shown in Figure 4.

### 3. SIMULATION AND EXPERIMENTAL RESULTS

#### 3.1. Simulation results

PSIM software with simplified C-Block are used to simulate the modified PWM technique optimized with the algorithms. According to Figure 1, the parameters of the NPC-MLI used in the simulation are shown in Table 1. To simplify the optimization, the injected signal is single waveform, and the frequency is determined manually. The frequency values are determined up to 21<sup>st</sup> harmonics. They are chosen to explore the best result from various value of injected frequency. Then, the amplitude and phase shift of the injected signal is optimized by GWO. Figure 5 shows an example of the tracking process results of injected signal with frequency of 650Hz. It can be seen from Figures 5(a) and 5(b), amplitude and phase shift injected

are searched initiated from zero then approached to best value. Figures 5(c) and 5(d) show the THD results from injected amplitude and phase shift. At time of around 6.1s, the best value of amplitude and phase shift are convergence.

Table 1. NPC-MLI simulation parameters

Components	Value
DC Source	311 V
Capacitor 1	270uF
Capacitor 2 Load	270uF 100 Ohm

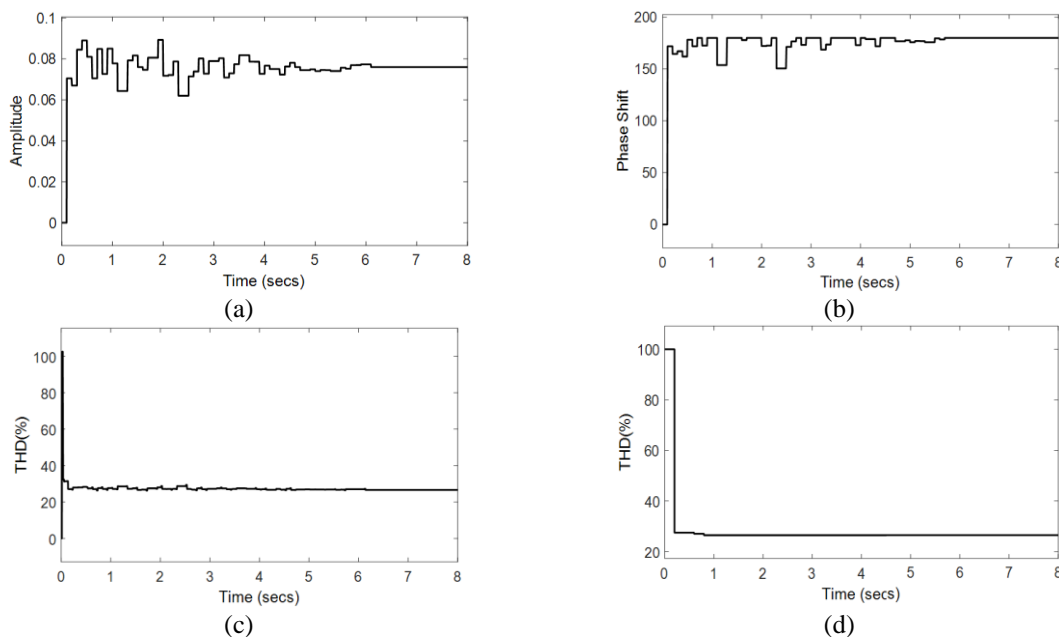


Figure 5. Simulation result in frequency 650Hz of optimized injected signal, (a) amplitude, (b) phase shift, (c) THD, and (d) the best THD reached

Optimization is performed to 10 various frequencies of injected signals. GWO is tested and compared its performance to other optimization methods, such as differential evolution (DE), human psychology optimization (HPO), and particle swarm optimization (PSO). Figure 6 shows comparison charts of the optimization results of the GWO, DE, HPO, and PSO algorithms. The charts show the best amplitude, the best phase shift, convergence time and the best THD. Convergence time in those charts mean the time needed to reach the best THD, such as shown in Figure 5(d). Convergence time is shown to represent the speed of optimization process. Figures 6(a) and 6(b) show the results of amplitude and phase shift. Figure 6(b) show clearly that GWO can find the best value of phase shift by avoiding trapped in local maxima. Contrarily, other algorithms trapped in local optima which indicated by extreme phase shift value of  $0^\circ$  or  $180^\circ$ . Consider to Figure 6(c), the lowest average THD is reached by GWO at 28.5%, then HPO 28.6%, DE 28.7% and PSO 28.8%. Figure 6(d) shows that DE is the slowest to convergence. Furthermore, the fastest average convergence time is reached by GWO at 6.079s then PSO 6.080s, HPO 6.164s and DE 37.118s. Figure 7 shows comparison of the THD minimization results plotted by time using GWO, DE, HPO and PSO at a frequency of 650Hz of injected signal. The injected signal resulted from GWO yielding a THD of 26.44%. The GWO process runs and finds the best solution in 6.14s. HPO yield THD of 26.61%, DE 26.62% and PSO 26.96%. HPO yield convergence time of 6.18s, PSO 6.44s and DE 37.8s.

Figures 8(a) and 8(b) shows the comparison of NPC-MLI output voltage waveform using SPWM and modified PWM. Since both of output voltage has same amplitude modulation, the injected signal effects to modified PWM can be identified by comparing the different pattern Figure 8(a) and 8(b). Figure 8(c) show clearly the THD level of modified PWM is lower than SPWM. Table 2 provides a comparison of the THD level of the NPC-MLI output voltage in percent. The SPWM has a THD of 31.42% and the modified PWM has a THD of 26.44%. Figure 9(a) experimental setup of proposed work and 9(b) hardware of NPC-MLI. Figure 10(a) harmonics spectrum of SPWM and 10(b) harmonics spectrum of modified PWM.

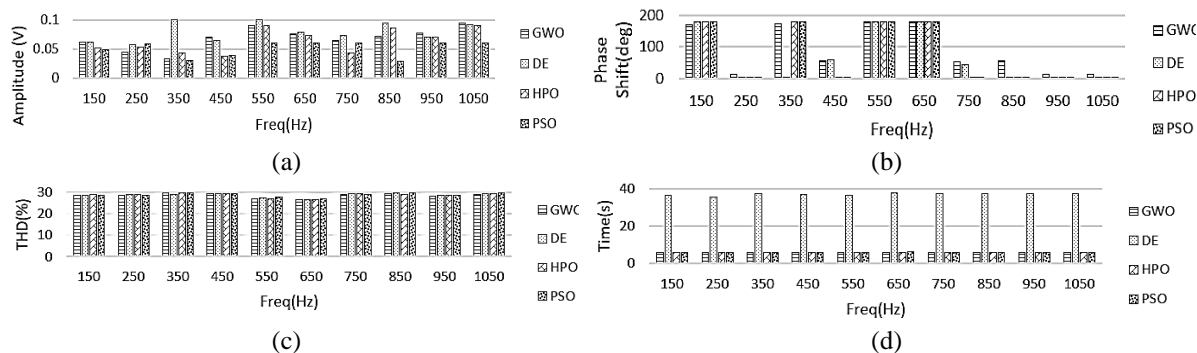


Figure 6. Optimization results from various algorithms, (a) amplitude (b) phase shift (c) THD, and (d) convergence time

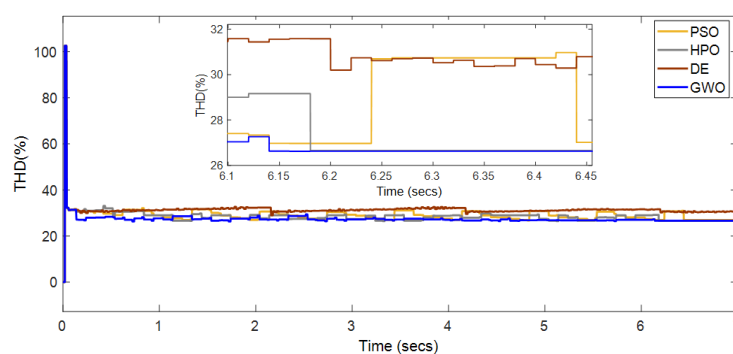


Figure 7. Comparison of the THD minimization results using GWO, DE, HPO and PSO at a frequency of 650 Hz of injected signal

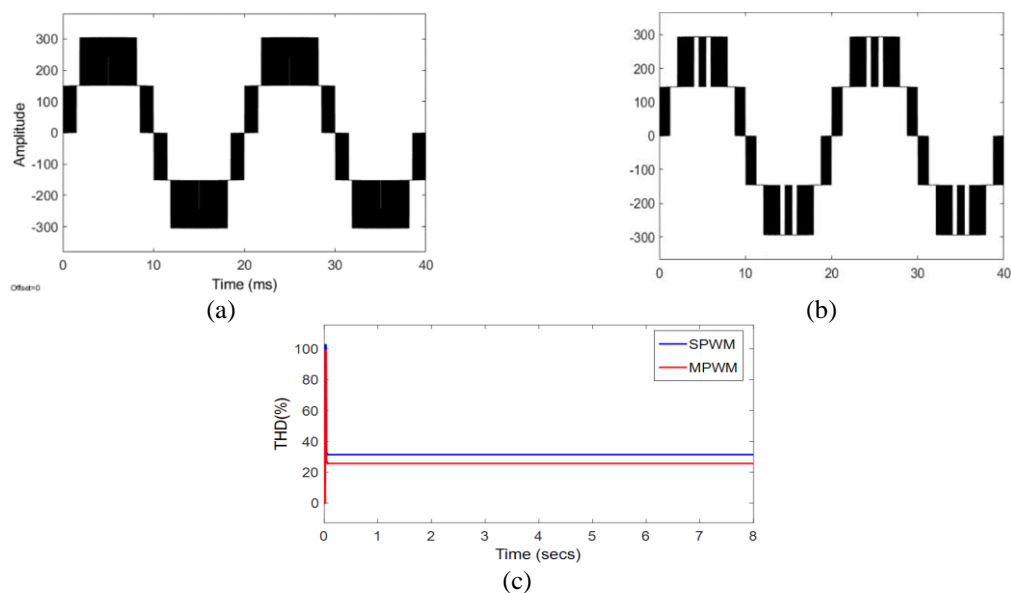


Figure 8. Output voltage of NPC-MLI, (a) SPWM, (b) modified PWM, and (c) SPWM THD and modified PWM THD on NPC-MLI in simulation

Table 2. THD comparison of modulation techniques in percent using simulation

Modulation Technique	THD (%)
SPWM	31.42
Modified PWM	26.44



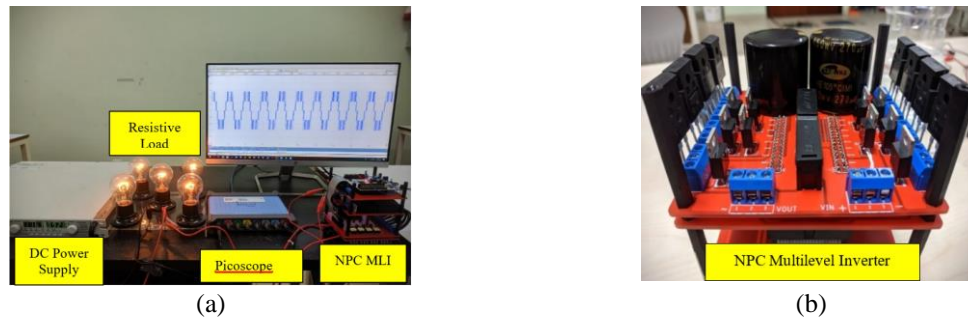


Figure 9. The result of the proposed work in hardware: (a) experimental setup and (b) NPC-MLI prototype

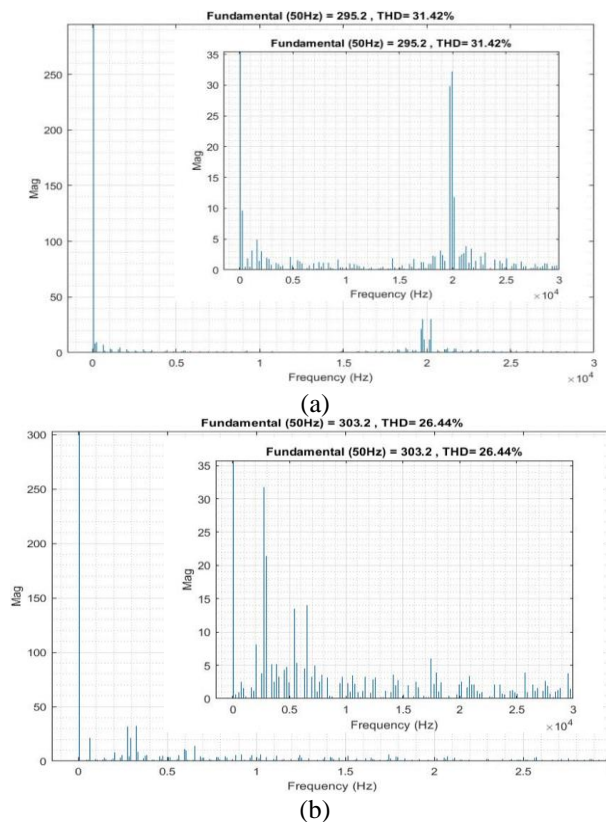


Figure 10. Harmonics spectrum: (a) SPWM and (b) modified PWM

### 3.2. Experimental results

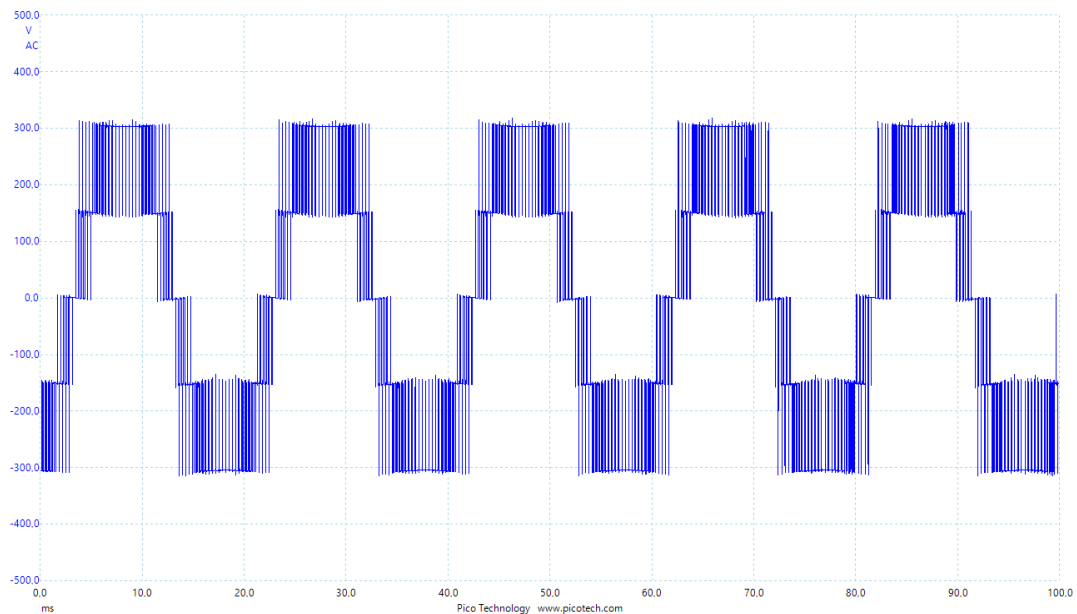
To verify the proposed modulation technique and to validate the simulation results achieved by GWO algorithm, a single-phase NPC-MLI prototype was built. Table 3 shows the components used to develop NPC-MLI. Figure 9(a) shows the setup of experimental system and Figure 9(b) shows the zoomed picture of NPC-MLI. The Nucleo STM32F446RE microcontroller is used to generate pulses for NPC-MLI switching. Picoscope is used to measure and to analyze the waveform, harmonics spectrum and THD. Programmable DC Power supply TDK-Lambda is used to provide constant DC voltage input of NPC-MLI. The NPC MLI is tested with an DC input voltage of 311 V and is loaded with a resistive load.

Table 3. Components used for experiment

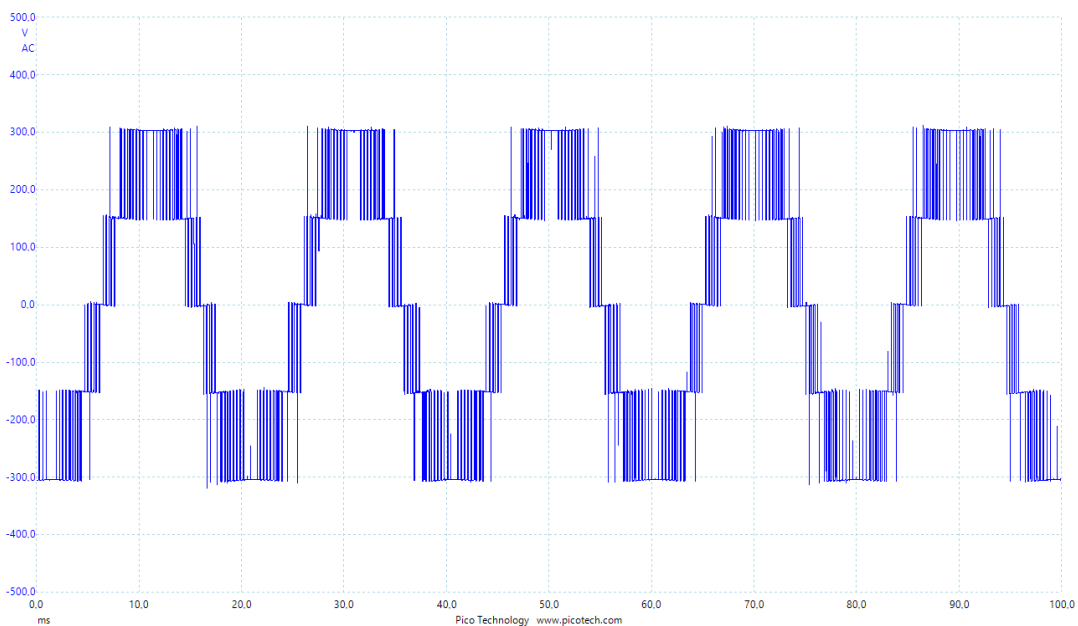
Components	Specifications
IGBT Module	K40H1203 (Infineon)
Microcontroller	Nucleo STM32F446RE
Optocoupler	FOD3182 (Fairchild)
Fast Diode	MUR 1560
Gate Driver Power Supply	DC 12V, HLK-PM12



NPC-MLI is operated to verify the modulation of SPWM and modified PWM technique with the best parameters from the simulation results. Both of SPWM and the modified PWM is set to amplitude modulation of 1. Furthermore, the modified PWM is injected by signal of 650Hz with an amplitude of 0.07519 and phase shift of 180 degrees. Figures 11(a) and 11(b) show the comparison results of experiments between output voltage of SPWM and modified PWM. The results are similar to simulation results as shown in Figure 8. The output voltage is recorded to determine the THD. Figure 12 shows the spectrum and THD results. Both of modulation produce harmonic spectrum at very low level and at high frequency. The high harmonics of frequency spectrum can be advantage for the suppression of distortion by only using small LC filter. From Figure 12, SPWM produces higher THD than modified PWM. Figure 12(a) shows the THD measurement using the spectrum mode of picoscope 4824 is 28.15%. Figure 12(b) shows the output waveform of a NPC-MLI using Modified PWM switching. The THD is noticeably less than SPWM. Figure 12(b) The measured THD is 26.4% which proves that switching Modified PWM optimized by GWO produced lower THD than SPWM.



(a)



(b)

Figure 11. Output voltage of NPC-MLI: (a) SPWM and (b) modified PWM



Figure 12. THD measurement using spectrum mode of picoscope 4824: (a) THD of SPWM and (b) THD of modified PWM on prototype system

#### 4. CONCLUSION





This paper presents modified PWM with optimization using the GWO algorithm as an alternative modulation technique to reduce voltage harmonics in NPC-MLI. The values of frequency, amplitude, and shift angle are optimized to produce low THD. The GWO algorithm is then compared to other algorithms such as DE, HPO and PSO to test their performance in harmonic reduction and convergence level. As a result, GWO can optimize modified PWM to obtain global optima with a minimum. To validate the proposed theory, a prototype has been built and tested to compare between common SPWM and Modified PWM optimized by GWO. The lower THD produced by proposed method can be applied to increase the performance of NPC-MLI. Furthermore, the low THD NPC-MLI can help to promote the next level of renewable energy applications.

#### REFERENCES





- [1] P. R. Bana, K. P. Panda, R. T. Naayagi, P. Siano and G. Panda, "Recently Developed Reduced Switch Multilevel Inverter for Renewable Energy Integration and Drives Application: Topologies, Comprehensive Analysis and Comparative Evaluation," *IEEE Access*, vol. 7, pp. 54888-54909, 2019, doi: 10.1109/ACCESS.2019.2913447.
- [2] K. P. Panda, S. S. Lee and G. Panda, "Reduced Switch Cascaded Multilevel Inverter With New Selective Harmonic Elimination Control for Standalone Renewable Energy System," *IEEE Transactions on Industry Applications*, vol. 55, no. 6, pp. 7561-7574, 2019, doi: 10.1109/TIA.2019.2904923.
- [3] V. F. Piresa, A. Cordeiroc, D. Foitoa, and J. F. Silva, "Three-phase MLI for grid-connected distributed photovoltaic systems based in three three-phase two-level MLIs," *Solar Energy*, vol. 17, no. 4, pp. 1026-1034, 2018, doi: 10.1016/j.solener.2018.09.083.
- [4] C. Liu *et al.*, "Hybrid SiC-Si DC-AC Topology: SHEPWM Si-IGBT Master Unit Handling High Power Integrated With Partial-Power SiC-MOSFET Slave Unit Improving Performance," *IEEE Transactions on Power Electronics*, vol. 37, no. 3, pp. 3085-3098, 2022, doi: 10.1109/TPEL.2021.3114322.

- [5] S. Maurya, D. Mishra, K. Singh, A. K. Mishra and Y. Pandey, "An Efficient Technique to reduce Total Harmonics Distortion in Cascaded H- Bridge Multilevel Inverter," *IEEE International Conference on Electrical, Computer and Communication Technologies (ICECCT)*, 2019, pp. 1-5, doi: 10.1109/ICECCT.2019.8869424.
- [6] S. Choudhury, M. Bajaj, T. Dash, S. Kamel and F. Jurado, "MLI: A Survey on Classical and Advanced Topologies, Control Schemes, Applications to Power System and Future Prospects," *Energies*, vol. 14, no. 5773, pp. 1-47, 2021, doi: 10.3390/en14185773.
- [7] P. Kala, and S. Arora, "A comprehensive study of classical and hybrid MLI topologies for renewable energy applications," *Renewable and Sustainable Energy Reviews*, vol. 76, pp. 905-931, 2017, doi: 10.1016/j.rser.2017.02.008.
- [8] B. Mahato, S. Majumdar, S. Vatsyayan and K.C. Jana, "A new and generalized structure of MLI topology with half-bridge cell with minimum number of power electronic devices," *IETE Technical Review*, vol. 38, no. 2, pp. 267-278, 2020, doi: 10.1080/02564602.2020.1726215.
- [9] L. Gang, W. Dafang, W. Miaoran, Z. Cheng and W. Mingyu, "Neutral-Point Voltage Balancing in Three-Level Inverters Using an Optimized Virtual Space Vector PWM With Reduced Commutations," *IEEE Transactions on Industrial Electronics*, vol. 65, no. 9, pp. 6959-6969, 2018, doi: 10.1109/TIE.2018.2798565.
- [10] V. Jayakumar, B. Chokkalingam and J. L. Munda, "A Comprehensive Review on Space Vector Modulation Techniques for Neutral Point Clamped Multi-Level Inverters," *IEEE Access*, vol. 9, pp. 112104-112144, 2021, doi: 10.1109/ACCESS.2021.3100346.
- [11] C. Bharatiraja, B. M. Sagar, P. Sanjeevikumar, V. K. Ramachandramurthy, and I. Atif, "Investigations of multi-carrier pulse width modulation schemes for diode free neutral point clamped multilevel inverters," *Journal of Power Electronics*, vol. 19, no. 3, pp. 702-713, 2019, doi: 10.6113/JPE.2019.19.3.702.
- [12] M. D. Siddique, S. Mekhilef, S. Padmanaban, M. A. Memon and C. Kumar, "Single-Phase Step-Up Switched-Capacitor-Based Multilevel Inverter Topology With SHEPWM," *IEEE Transactions on Industry Applications*, vol. 57, no. 3, pp. 3107-3119, 2021, doi: 10.1109/TIA.2020.3002182.
- [13] P. Madasamy *et al.*, "A simple multilevel space vector modulation technique and MATLAB system generator built FPGA implementation for three-level neutral-point clamped inverter," *Energies*, vol. 12, no. 22, pp. 1-24, 2019, doi: 10.3390/en12224332.
- [14] S. Singh, A. Agnihotri, S. Bind and S. Kumar, "Matlab Simulation Study and Comparison of Different Multiple Carrier PWM Schemes For Multi Level CHB Inverter," *IEEE First International Conference on Smart Technologies for Power, Energy and Control (STPEC)*, 2020, pp. 1-6, doi: 10.1109/STPEC49749.2020.9297693.
- [15] A. Pourdashnia, M. Sadoughi, M. Farhadi-Kangarlou and B. Tousi, "Selective Harmonic Elimination in a Cascaded H-Bridge Multilevel Inverter fed by High-Frequency Isolated DC-DC Converter," *IEEE Kansas Power and Energy Conference (KPEC)*, 2021, pp. 1-5, doi: 10.1109/KPEC51835.2021.9446223.
- [16] Mohammad Sadegh Orfi Yeganeh, Mohammad Sarvi, Frede Blaabjerg, and Pooya Davari, "Improved harmonic injection pulse-width modulation variable frequency triangular carrier scheme for multilevel inverters," *IET Power Electronics*, vol. 13, no. 14, pp. 3146-3154, 2020, doi: 10.1049/iet-pel.2020.0232.
- [17] A. A. H. Eldin, E. Negm, M. S. Elgama, and K. M. AboRas, "Operation of grid-connected DFIG using SPWM-and THIPWM-based diode-clamped multilevel inverters," *IET Generation, Transmission & Distribution*, vol. 14, no. 8, pp. 1412-1419, 2020, doi: 10.1049/iet-gtd.2019.0248.
- [18] N. Ziling, W. Ye, J. Zhu, and J. Xu, "Capacitor voltage feedforward decoupling control based on third harmonic injection modulation for five-level active neutral point clamped converter," *Journal of Power Electronics* vol. 20, no. 6, pp. 1638-1649, 2020, doi: 10.1007/s43236-020-00136-1.
- [19] A. S. Kumar, K. S. Gowri and M. V. Kumar, "Performance study of various discontinuous PWM strategies for multilevel inverters using generalized space vector algorithm," *Journal of Power Electronics*, vol. 20, no. 1, pp. 100-108, 2020, doi: 10.1007/s43236-019-00010-9.
- [20] M. A. Memon, S. Mekhilef, M. Mubin, and M. Aamir, "Selective harmonic elimination in MLIs using bio-inspired intelligent algorithms for renewable energy conversion applications: A review," *Renewable and Sustainable Energy Reviews*, vol. 82, no. 3, pp. 2235-2253, 2018, doi: 10.1016/j.rser.2017.08.068.
- [21] A. K. V. K. Reddy and K. V. L. Narayana, "Optimal total harmonic distortion minimization in multilevel inverter using improved whale optimization algorithm," *International Journal of Emerging Electric Power Systems*, vol. 21, no. 3, pp. 1-25, 2020, doi: 10.1515/ijeeps-2020-0008.
- [22] W. T. Chew, W. V. Yong, S. L. Ong and J. H. Leong, "Harmonics Minimization in MLI Using Grasshopper Optimization Algorithm," *International Journal of Electronics*, vol. 109, no. 6, pp. 1009-1034, doi: 10.1080/00207217.2021.1966660.
- [23] A. A. K. Arani, H. Karami, B. Vahidi, and G. B. Gharehpetian, "Improved hyper-spherical search algorithm for voltage total harmonic distortion minimization in 27-level inverter," *Journal of Central South University*, vol. 26, no. 10, pp. 2822-2832, 2019, doi: 10.1007/s11771-019-4216-2.
- [24] L. P. S. Raharja, Q. A. Ony, Z. Arief and N. A. Windarko, "Reduction of Total Harmonic Distortion (THD) on Multilevel Inverter with Modified PWM using Genetic Algorithm," *Emitter International Journal of Engineering Technology*, vol. 5, no. 1, pp. 91-118, 2017, doi: 10.24003/emitter.v5i1.174.
- [25] E. F. Firmansyah, O. A. Qudsi, M. N. Habibi and N. A. Windarko, "Optimized Modified PWM based on Differential Evolution for Reducing THD on Multilevel Inverter," *International Seminar on Intelligent Technology and Its Applications (ISITIA)*, 2020, pp. 113-118, doi: 10.1109/ISITIA49792.2020.9163729.
- [26] D. J. Hemanth, and J. Anitha, "Modified Genetic Algorithm approaches for classification of abnormal Magnetic Resonance Brain tumour images," *Applied Soft Computing*, vol. 75, pp. 21-28, 2019, doi: 10.1016/j.asoc.2018.10.054.
- [27] A. W. Mohamed, and P. N. Suganthan, "Real-parameter unconstrained optimization based on enhanced fitness-adaptive differential evolution algorithm with novel mutation," *Soft Computing*, vol. 22, no. 10, pp. 3215-3235, 2018, doi: 10.1007/s00500-017-2777-2.
- [28] S. Mirjalili, S. M. Mirjalili, and A. Lewis, "Grey Wolf Optimizer," *Advances in Engineering Software*, vol. 69, pp. 46-61, 2014, doi: 10.1016/j.advengsoft.2013.12.007.





**BIOGRAPHIES OF AUTHORS**

**Fahmi Ahyar Izzaqi**     is an undergraduate student in Electrical Engineering Department at Politeknik Elektronika Negeri Surabaya, Indonesia, since 2018. He became head of the research and technology department at the student association in 2019 and a member of Renewable Energy Research Centre of PENS 2021. Previously, he attended a vocational high school 2 Salatiga, in the same field that is electrical engineering. Now, he is interested in power quality, renewable energy and artificial intelligence. His first paper discusses about it and is expected to be an inspiration for other researchers to be better developed. He can be contacted at email: fahmizzaqi@gmail.com or fahmizzaqi@pe.student.pens.ac.id.



**Novie Ayub Windarko**     finished his bachelor and master degree from Department of Electrical Engineering, Institut Teknologi Sepuluh Nopember Surabaya, Indonesia. He received his Ph.D from School of Electrical Engineering, Chungbuk National University, South Korea. He has been joining to PENS since 2000. He was a JICA junior visiting researcher in Hirofumi Akagi Lab., Tokyo Institute of Technology in 2002. He was the head of Renewable Energy Research Centre of PENS. He received the best paper and the best poster award at IEEE IES 2015. His research interests include power electronics converter, PV power generation and optimization for renewable energy. He can be contacted at email: ayub@pens.id.



**Ony Asrarul Qudsi**     was born in Probolinggo, Indonesia on June 15, 1990. The author completed his bachelor's degree in 2012 at Institut Teknologi Sepuluh Nopember. Then the author continued his Master's Education at Institut Teknologi Sepuluh Nopember, Surabaya, Indonesia. The author completed the Master's program in 2014. He was joined Politeknik Elektronika Negeri Surabaya, Indonesia in 2013 as lecture. The author's love for the concentration of the Power System Engineering, made the author do a lot of research and publicize both journals and seminars in the field of Power Systems Engineering. He can be contacted at email: ony@pens.ac.id.